

Paul J. Neiman<sup>1\*</sup>, F.M. Ralph<sup>1</sup>, A.B. White<sup>2</sup>, D.E. Kingsmill<sup>3</sup>, P.O.G. Persson<sup>2</sup><sup>1</sup>NOAA/ Environmental Technology Laboratory, Boulder, Colorado<sup>2</sup>Cooperative Institute for Research in Environmental Sciences/NOAA/ETL, Boulder, Colorado<sup>3</sup>Desert Research Institute, Reno, Nevada

## 1. INTRODUCTION

During a typical winter, many mountain ranges of the western United States are inundated with copious amounts of orographically enhanced precipitation. Perhaps the largest of these ranges is the Sierra Nevada of California, reaching an altitude of >4 km above mean sea level (MSL) and extending horizontally for over 600 km. Because California depends on runoff from the Sierras for its water supply and power generation, numerous investigators (e.g., Heggli and Rauber 1988; Pandey et al. 1999) have studied wintertime orographic precipitation associated with this lofty and lengthy mountain range. Though far less dramatic than the Sierras, California's coastal mountain ranges also generate significant orographic precipitation. These modest ranges are typically <100 km long and extend upward to only ~500-1500 m MSL, but they can generate orographically-induced floods during the land-fall of winter storms, incurring millions of dollars in property damage and fatalities (e.g., NOAA 1982, 1998). As California's coastal population continues to blossom, orographic floods generated by these mountains pose an increasing threat. Motivated by this threat, the California Land-falling Jets Experiment (CALJET; Ralph et al. 1999) was carried out during the winter of 1997-98.

Our study quantitatively links rainfall rates in California's coastal mountains to upslope flow measured immediately upstream along the coast during CALJET, using hourly wind-profiler and rain-gauge data from an integrated observing network northwest of San Francisco (Fig. 1). Because of the availability of these wind profiles, we were able to determine the layer of upslope flow that optimally modulates mountain rainfall, and we could assess the sensitivity of mountain rain rates to low-level jet (LLJ) conditions.

## 2. LAND-BASED OBSERVING SYSTEMS AND METHODOLOGY

This observing network consisted of a 915-MHz wind profiler and rain gauge deployed along the coast (BBY), and another set deployed in the coastal mountains (CZD), by the NOAA's Environmental Technology Laboratory (Fig. 1). The profilers measured hourly wind profiles with ~100-m resolution from ~0.1 to 4.0 km, well above the highest coastal terrain. Wind data from collocated surface meteorological towers extended the hourly wind profiles down to the surface. The tipping-bucket gauges measured rainfall every 2 min with 0.01-inch (~0.25 mm) resolution. In this conference presentation, we utilize the coastal wind-profiler and mountain rain-gauge data.

Predicated on basic theoretical concepts relating horizontal moisture convergence to orographic precipitation, and assuming two-dimensionality, a least-squares linear regression fit was applied to

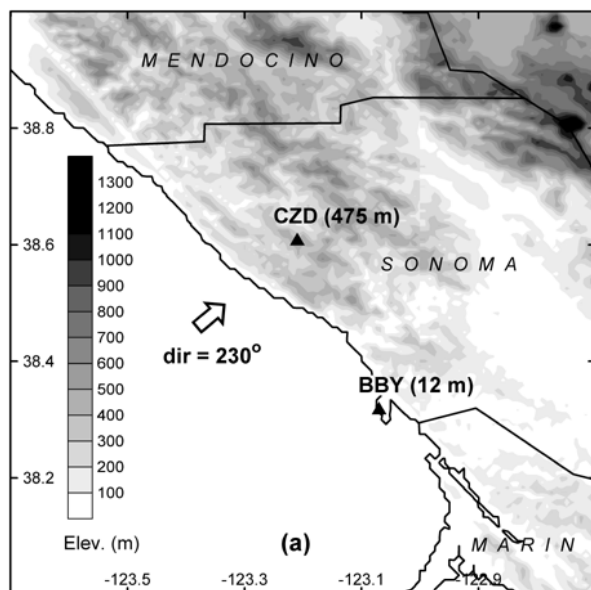


Fig. 1. Terrain base map showing the 915-MHz wind-profiler/rain-gauge sites at BBY and CZD. The site elevations, and the vector portraying the flow direction most nearly perpendicular to the mountain barrier, are shown. Counties are labeled.

measurements of upslope flow at each 500-m-thick vertically averaged layer (and at the surface) and corresponding observations of rain rate measured in the downstream coastal mountains. This approach yielded a vertical profile of correlation coefficient for the CALJET winter season. A total of 468 hourly data points were used to obtain the winter-season correlation profile, which will be described later in the context of the low-level jet results. It should be noted that factors other than the magnitude of the upslope flow can also affect the intensity of orographic precipitation, including available moisture supply, thermodynamic stratification, and the release of potential instability. Because we did not launch frequent thermodynamic soundings during CALJET, this study is not fully able to link these factors to rain rates observed in the coastal mountains.

## 3. RESULTS

A focal point of CALJET's observing strategy was to document the structure and physical processes in the LLJ region ahead of land-falling cold fronts over the eastern

\*Corresponding author address: Paul J. Neiman, NOAA/ETL; 325 Broadway, Boulder, CO 80305; email: Paul.J.Neiman@noaa.gov

Pacific, because it is believed that land-falling LLJs contribute to heavy orographic rainfall as they impact the windward slopes of coastal mountains (e.g., Browning et al. 1975). During CALJET, a prominent LLJ was observed by NOAA's P-3 research aircraft during ten flights well offshore of California, where terrain effects were negligible. Composite profiles of wind velocity and moisture through the LLJ were generated (Fig. 2) using flight-level and dropsonde observations from those flights. The composite wind-speed profile contains a LLJ of  $\sim 31$   $\text{m s}^{-1}$  centered at about 0.9 km MSL. The companion wind-direction profile veers with height from south-southwesterly near the ocean surface to southwesterly above the LLJ at  $\sim 2$  km. The composite water-vapor mixing ratio profile shows moist conditions ( $\sim 10$   $\text{g kg}^{-1}$ ) below  $\sim 300$  m MSL, and a steady decrease of moisture with height aloft.

Despite the presence of well-defined LLJ characteristics over the open ocean, are LLJs readily observable at the coast or do they dissipate prior to land-fall because of terrain blocking and enhanced friction in the coastal zone? If LLJs make land-fall, do they modulate rainfall in California's coastal mountains? To answer these questions, we inspected the BBY profiler data from each of 25 rain cases totalling 468 h of data for evidence of a land-falling LLJ. We defined a LLJ as a maximum of total wind speed below 1.5 km MSL residing beneath a local minimum aloft. This low-level maximum was required to be at least 2  $\text{m s}^{-1}$  larger than the minimum aloft. At least two consecutive hourly profiles meeting these criteria were required to generate a mean wind profile representative of a LLJ for that case. Based on these criteria, eighteen of the 25 cases contained a

LLJ episode, totaling 81 hours of data. Composite wind speed, wind direction, and upslope-flow profiles were constructed (Fig. 3) from these 18 LLJ events. The composite wind-speed profile contains a LLJ of nearly 18  $\text{m s}^{-1}$  at  $\sim 1$  km MSL, or only  $\sim 100$  m above that of the offshore composite (Fig. 2). However, the core speed within the coastal LLJ composite is  $<60$  percent of the magnitude of its offshore counterpart. Some of this difference may have arisen because the coastal and offshore composites were composed of different populations of LLJs, and because the P-3 flights from which the offshore composite was derived focused on the strongest events. It is also possible that at least part of this reduction in speed arose through enhanced frictional effects in the coastal zone. The composite wind-direction profile at BBY is rotated counter-clockwise by  $\sim 25$  deg below mean mountain top relative to its offshore counterpart, thus suggesting that the coastal mountains may have deflected the low-level flow below jet level to a nearly terrain-parallel orientation. The composite upslope-flow profile contains a local maximum of  $\sim 14$   $\text{m s}^{-1}$  at about the height of the composite LLJ and above the shallow terrain-deflected flow.

To assess the impact of land-falling LLJs on rain rate in California's coastal mountains, the 81 h of profiler and rain-rate data from the LLJ inventory at the northern couplet were used to calculate vertical profiles of linear correlation coefficient and linear regression slope for the LLJ environment (Figs. 4 and 5). The vertical structure of the correlation coefficient profile (Fig. 4) mirrored that of the correlation coefficient profile based on the 468-h, 25-case winter-season inventory, i.e., a prominent maximum at 0.95 km MSL at the altitude of the LLJ flanked by much

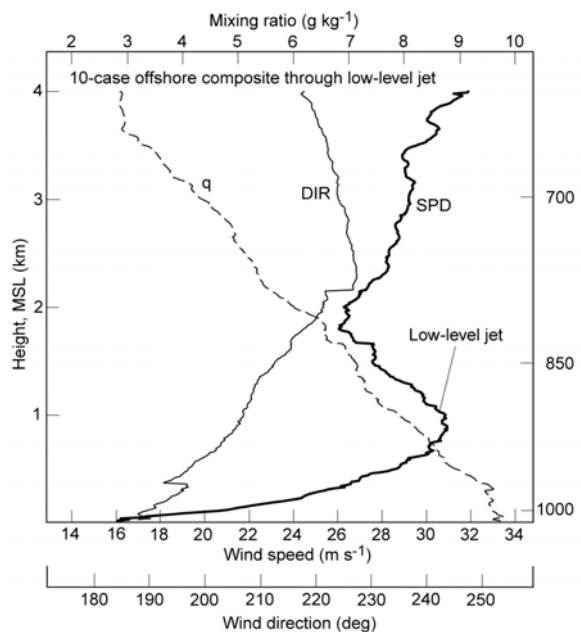


Fig. 2. Composite vertical profiles of wind speed (SPD), wind direction (DIR), and water-vapor mixing ratio ( $q$ ) based on NOAA P-3 flight-level and dropsonde measurements taken over the eastern Pacific during 10 CALJET storms that contained a low-level jet.

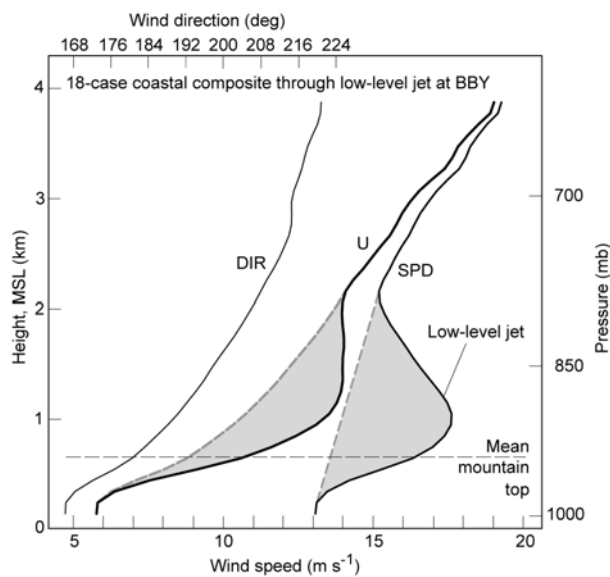


Fig. 3. Composite vertical profiles of wind speed (SPD), wind direction (DIR), and upslope flow (U) based on an average of the 18 CALJET cases from BBY that contained a low-level jet. The shaded regions portray the SPD and U perturbations associated with the low-level jet. The mean mountain-top height of the neighboring coastal mountains is shown.

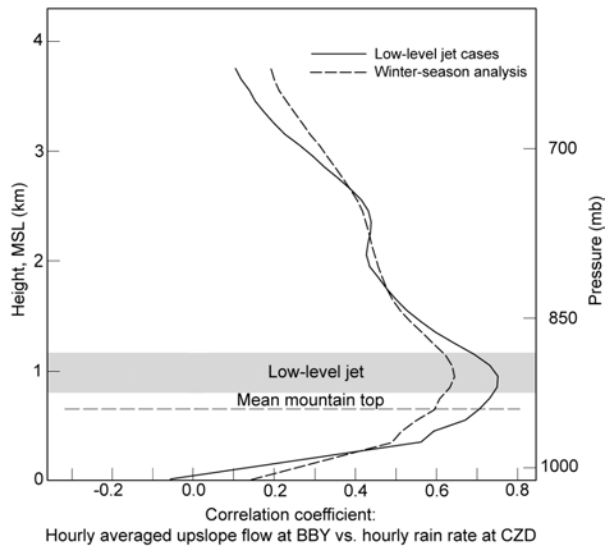


Fig. 4. Vertical profiles of linear correlation coefficient based on hourly profiles of upslope flow at BBY versus hourly rain rate at CZD for the 18 low-level jet cases (solid) and for the 25-case winter-season inventory (dashed). The shaded region denotes the position of the low-level jet. The mean mountain-top height of the neighboring coastal mountains is shown.

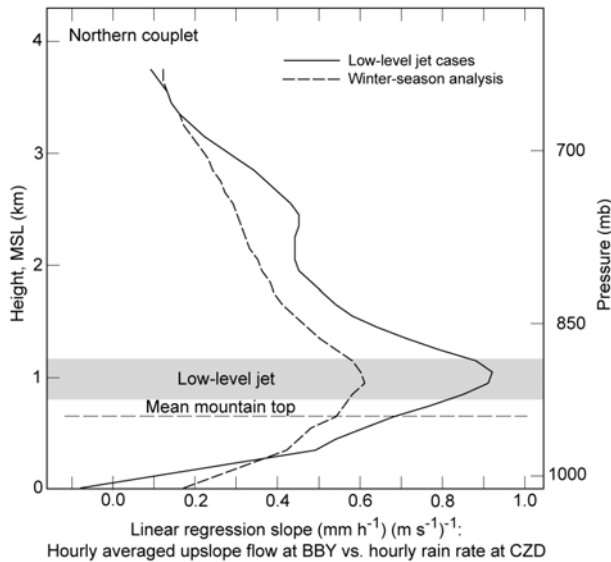


Fig. 5. Vertical profiles of linear regression slope based on hourly profiles of upslope flow at BBY versus hourly rain rate at CZD for the 18 low-level jet cases (solid) and for the 25-case winter-season inventory (dashed). The horizontal shaded bar and dashed line are as in Fig. 4.

lower values. Significantly, the maximum correlation coefficient increased from 0.644 based on the winter-season inventory to 0.751 for the LLJ subsample, thus indicating that the linear relationship between upslope flow and rain rate is more robust in LLJ conditions than for the less restrictive winter-season inventory. The profiles of linear regression slope for the LLJ and winter-season inventories (Fig. 5) show a jet-level maximum of  $0.92 \text{ mm h}^{-1} [\text{m s}^{-1}]^{-1}$  for the LLJ subsample that is approximately 50 percent steeper than for the winter-season inventory. Because the LLJ inventory yields a substantially more efficient rain-rate response at jet level than the winter-season inventory for a given increase in upslope flow, it is likely that the LLJ environment possessed more favorable thermodynamics (e.g., greater low-level moisture and larger potential instability) that allowed heavier orographic rains to develop and persist over the mountains during periods of enhanced upslope flow. A comparison of average rainfall characteristics between the LLJ and winter-season inventories support this assertion: the rain rate at CZD was 47 percent larger during the LLJ cases and the rainfall ratio between CZD and BBY was 13 percent larger.

The orographic rain-rate enhancement at CZD associated with the composite LLJ profile at BBY was estimated, based on the assumption that the composite LLJ and its upslope maximum is a perturbation from a mean state that is devoid of the LLJ. A vertical profile of rain-rate enhancement was calculated (Fig. 6) by multiplying the upslope perturbation at each level (Fig. 3) with the LLJ-based linear regression slope at the same altitude (Fig. 5). Because the upslope-flow perturbation is largest at the height of the LLJ and at the height of the steepest regression slope, the orographic rain-rate enhancement is also maximized at the altitude of the LLJ. This is also the altitude where the linear relationship between upslope flow at BBY and rain rate at CZD is statistically most robust. Though the maximum rain-rate

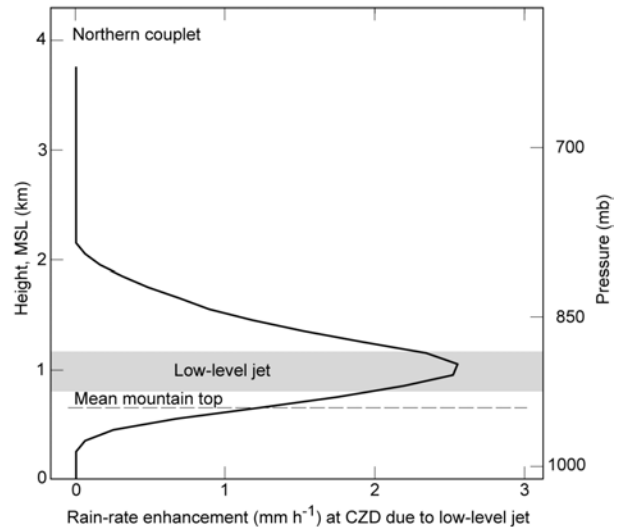


Fig. 6. Vertical profile of rain-rate enhancement at CZD based on the 18-case low-level jet composite at BBY. The horizontal shaded bar and dashed line are as in Fig. 4.

enhancement of  $2.55 \text{ mm h}^{-1}$  (Fig. 6) is not exceptionally large, it does represent 57 percent of the average rain rate of  $4.50 \text{ mm h}^{-1}$  at CZD for the LLJ inventory (or a total of 206 mm of rainfall) and 83 percent of the average rain rate of  $3.07 \text{ mm h}^{-1}$  at CZD for the less restrictive winter-season inventory. Furthermore, persistent LLJ events can yield significant rainfall amounts. Finally, individual events possessing a much larger LLJ perturbation than the composite can yield much greater rain rates associated with the LLJ. It should also be noted that the migration of LLJs into the coastal mountains should provide a temporal increase of upslope flow regardless of the vertical structure of the wind profile, thus yielding an additional rain-rate enhancement, though that topic of research is not covered in this paper. We plan to further explore the relationship between the LLJ environment and orographic rainfall in future research.

## REFERENCES

- Browning, K.A., C.W. Pardoe, and F.F. Hill, 1975: The nature of orographic rain at wintertime cold fronts. *Quart. J. Roy. Meteor. Soc.*, **101**, 333-352.
- Heggli, M.F., and R.M. Rauber, 1988: The characteristics and evolution of supercooled water in wintertime storms over the Sierra Nevada: A summary of microwave radiometric measurements taken during the Sierra Cooperative Pilot Project. *J. Appl. Meteor.*, **27**, 989-1015.
- NOAA, 1982: *Storm Data*. Vol. 24. National Climatic Data Center. 31 pp.
- NOAA, 1998: *Storm Data*. Vol. 40. National Climatic Data Center. 188 pp.
- Pandey, G.R., D.R. Cayan, and Konstantine P. Georgakakos, 1999: Precipitation structure in the Sierra Nevada of California during winter. *J. Geophys. Res.*, **104**, 12019-12030.
- Ralph, F.M., and Coauthors, 1999: The California Land-falling Jets Experiment (CALJET): Objectives and design of a coastal atmosphere-ocean observing system deployed during a strong El Niño. Preprints, *Third Symp. on Integrated Observing Systems*, Dallas, TX, Amer. Meteor. Soc., 78-81.